Integration of the EMT-H Water Conduit Model with the Turbine Control System for Power System Dynamics

Ravi P. Mutukutti, José R. Martí

***Abstract*—Travelling pressure waves in hydraulic pipes in hydro generators can cause pressure transients that can implode or explode the pipes. These transients in the pipes limit the speed at which the mechanical power can be increased or decreased to compensate for transients in the electrical system. This paper uses the EMT-H hydraulic transients model developed in previous work in conjunction with the governor controller to more effectively dampen the electrical power system dynamics by coordinating the water transients with the electrical transients without damaging the pipes. The solution of EMT-H is very fast and can be incorporated into the control loop of the traditional controllers for an improved response. To test the new controller, the IEEE nine-bus, three-machine power system is used to solve a frequency stability problem during sudden load changes. From the hydraulic dynamics, we make observations on the adverse effects of the newer power-droop governor controllers compared to the traditional gate-droop controller and propose a new hybrid controller. We also consider pooling of control loops of companion plants to improve the overall dynamics of the combined responses. Improved plant control dynamics are becoming more important with the decrease of mechanical inertia in IBR systems.**

***Keywords*: EMT-H hydraulic equations, gate droop versus power droop controllers, hydro turbine governors, power system transient stability.**

I. Introduction

HYDRO generators produce a significant portion of the electric energy supply. The electrical power produced by a hydro generator depends on the water pressure and flow dynamics of the water feeding the turbine. The elasticity of the water and the conduit creates travelling waves that result in local over- and under-pressure sections (water hammer) when the supply of water reacts to a change in the electrical power demand. The speed of propagation of the water travelling waves is about 1200 m/s [1] [2], and the plants with long water conduits are particularly sensitive. Normally, in power system transient stability studies, it is assumed that the position of the wicket gate controlling the water flow to the turbine generator (mechanical power input) either does not change during the transient or that the mechanical shaft torque is proportional to the wicket gate position, ignoring the water conduit dynamics.

Because of the uncertainty in estimating the pressure transients in the pipes, conservative tolerance margins are set in the wicket gate opening and closing rates to safeguard the integrity of the pipes. These conservative tolerance limits, however, hinder a quicker response to the electrical system dynamics.

In [3], we introduced the EMT-H model, which is capable of modelling the transient hydraulic dynamics in real-time control applications. The EMT-H model uses the equations of the EMT transmission line models to model the water waves.

The validity of the proposed hydraulic model was proven in [3] by comparing the results with a field test on one of the BC Hydro power plants [3]. For this case, the proposed model was two orders of magnitude faster than the finite differences model while giving an overall similar accuracy.

In the present paper, we combine the equations of the EMT-H model with the electrical equations for power system transient stability studies to integrate governor control of the mechanical power with the flow of electrical power to better control power system dynamics without exceeding the limits of the turbine's wicket gate.

The IEEE 9-bus power system was used to study the frequency deviations to a step disturbance in the load is studied. Including the EMT-H equations in the governor control equations improves the nadir point of the oscillations and the settling characteristics of the transients. In addition, we observe the adverse effects caused by the latest approaches to fixing the power droop in modern-day electronic governors instead of using the historical gate droop control.

We also suggest a strategy to improve the response of hydraulic plants with long water conduits by teaming up this plant with a compensating controller at a companion conjugate plant. In the future, coordinated global control among multiple plants can strengthen the robustness of the AC system to compensate for the mechanical inertia loss due to the penetration of inverter-based generation.

This paper is organized as follows. We first review the companion EMT-H equations for hydraulic pipes and their validity compared to the finite differences model normally used for hydraulic transients. We then combine the EMT-H model with a transient stability model to study a number of frequency stability cases. We show that, particularly for long hydraulic pipes, using the EMT-H model can have a strong influence on

This work was supported in part by The Natural Sciences and Engineering Research Council of Canada (NSERC)

R. P. Mutukutti is with British Columbia Hydro (BC Hydro), Burnaby, BC, Canada (email: ravi.mutukutti@bchydro.com).

J. R. Marti is with the Department of Electrical Engineering, University of British Columbia, Vancouver, BC, Canada (the corresponding author's email is jrms@ece.ubc.ca).

Paper submitted to the International Conference on Power Systems Transients (IPST2025) in Guadalajara, Mexico, June 8-12, 2025.

the predicted electric power dynamics.

II. The EMT-H Model

In [3], using the second-order partial differential equations of propagation, we derived the water flow equations in hydraulic conduits as analogous to the well-known EMT transmission line models [6].

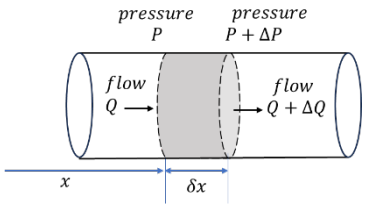

Fig. 1. Elementary segment of an elastic water (hydraulic) conduit.

Fig. 1 shows a slightly compressible fluid in a conduit with linearly elastic walls. The partial differential equations that relate pressure (P) and flow (Q) can be expressed [1] as,

$$-\frac{\partial Q}{\partial x} = \frac{A}{\rho a^2}\frac{\partial P}{\partial t} \tag{1}$$

and,

$$-\frac{\partial P}{\partial x} = \frac{\rho f}{2DA^2}|Q|Q + \frac{\rho}{A}\frac{\partial Q}{\partial t} \tag{2}$$

where Q is the fluid flow in cubic meters per second, P is the pressure of the fluid in pascals, t is the time in seconds, x is the distance along the fluid conduit in meters, A is the cross-sectional area of the conduit in square meters, ρ is the density of the fluid in kilograms per cubic meter, f is the non-dimensional Darcy-Weisbach friction factor, a is the celerity (wave speed) of the water in the conduit in meters per second, and D is the diameter of the hydraulic conduit in meters.

Korteweg's equation for the wave velocity (celerity) a is given by Halliwell [2] as,

$$a = \sqrt{1/\rho\left[\frac{1}{K} + \frac{\varphi}{E}\right]} \tag{3}$$

where K is the Bulk Modulus of Elasticity of the fluid in pascals, ρ is the density of the fluid in kilograms per cubic meter, E is Young's modulus of elasticity of the conduit walls in pascals, and φ is a non-dimensional parameter that depends on the conduit's arrangement such as anchoring and its dimensions. The value of φ for a thin-walled conduit with frequent expansion joints is given by D/e, where D is the diameter and e is the wall thickness both in meters [1].

By comparing (1) and (2) with the corresponding current and voltage relationships of Fig. 2, an analogy can be established between the hydraulic parameters and the electrical line parameters as follows. Defining C_{hy}, R_{hy} and L_{hy} as the hydraulic companion model parameters:

$$C_{hy} = \frac{A}{\rho a^2} = A\left[\frac{1}{K} + \frac{\varphi}{E}\right], \tag{4}$$

$$R_{hy} = \frac{f\rho}{2DA^2}|Q|, \tag{5}$$

$$L_{hy} = \frac{\rho}{A}. \tag{6}$$

Under this correspondence, the wave propagation speed, given by $a = \pm\sqrt{1/L_{hy}C_{hy}}$ in the electrical line coincides with Korteweg's Equation (3) for celerity in the fluid conduit. With (4)-(6), the fluid wave propagation problem can be expressed using an electrical transmission line model.

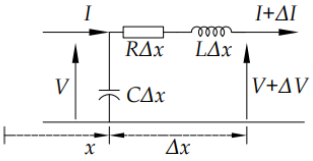

Fig. 2. Elementary segment of an electrical transmission line.

There are some limits to this correspondence. As opposed to the electrical line, the hydraulic resistance $R_{hy} = \frac{f\rho}{2DA^2}|Q|$ in (5) is flow (Q) dependent, while in the line, R is normally assumed as constant with respect to the flow I (even though it does depend on I indirectly by increasing the temperature of the conductor). It can be seen in Fig. 4 that using a constant resistance R_{hy}, at its steady-state value before the transient does not introduce much error in the fluid propagation results (at least for the cases studied in this paper).

III. The EMT-H Companion Model

The basic constant-parameter line model in the EMT (cpLine) was introduced by Dommel in [4] and represented a large improvement in accuracy and solution time over cascaded π sections of R, L, C parameters. In results presented in [6], it was shown that cpLine gives more accurate results than those obtained with 32 cascaded π's for a 320 km transmission line. Nonetheless, cpLine is about 50-100 times faster than the cascaded π's models. In [3], similar performance improvements were found between the EMT-H model and the traditional finite-differences models used in hydraulic transients.

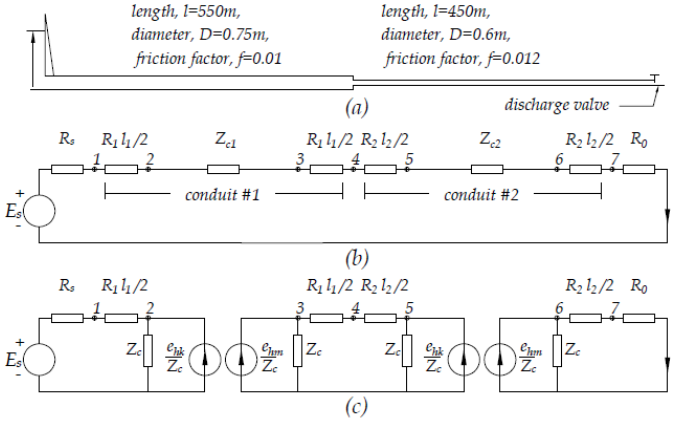

Fig. 3. EMT-H model of a dual-pipe hydraulic conduit (a) physical representation (b) EMT-H transmission line representation (c) decoupling using the cpLine model.

Fig. 3 shows the EMT-H model for two sections of hydraulic conduit using the proposed cpLine companion model. The

results from opening the discharge valve are shown in Fig. 4 from [3]. The EMT-H results are very similar to the finite differences (FD) model despite the fact that EMT-H was one hundred times faster. The computational speed of EMT-H makes it suitable for real-time control of governor controllers.

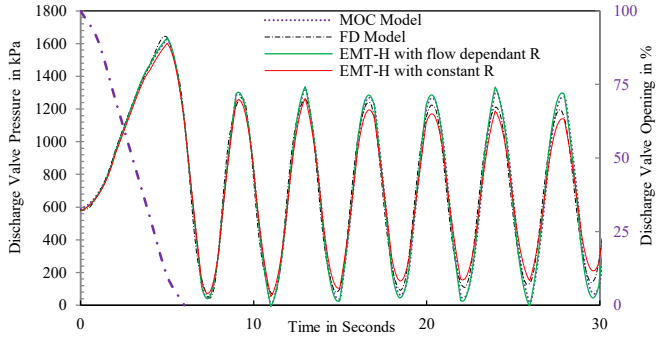

Fig. 4. Comparison of MOC, FD, and EMT-H solutions for the test in [3].

IV. Power System Stability with the EMT-H Companion Model

The IEEE nine-bus, three-machine power system [10], shown in Fig. 5, was used to test the effect of including the hydraulic transients in modelling power system dynamics. The power system parameters for the case are shown in Table I. The network's dynamic response of the system frequency is observed by applying a step load of 0.1 pu to Station B, Bus 6.

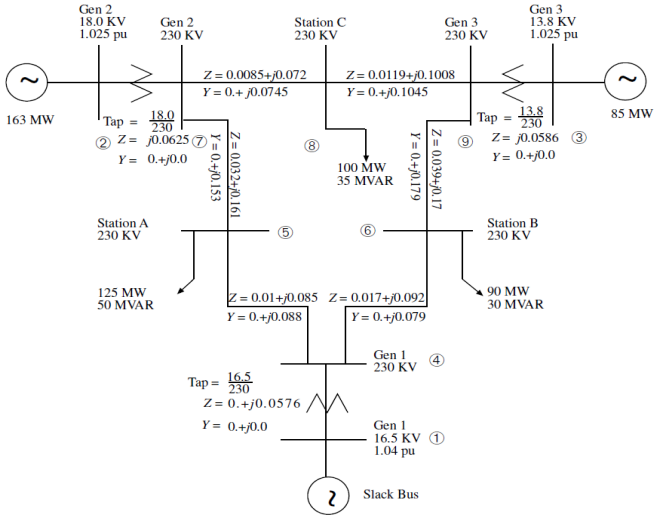

Fig. 5. IEEE nine-bus, three-machine power system modelled using traditional machine dynamic equations and the proposed EMT-H model for the hydraulic transients.

For the combined solution of the power system dynamics, including the hydraulic transient, we combined the equations of a transient stability model of the power system with the hydraulic equations. The hydraulic equations include: a) the EMT-H conduit model, (b) the wicket gate and mechanical power equations of the water turbine, (c) the generator, and (d) the network power flow equations.

A. Hydraulic Conduit

The EMT-H model calculates the water pressure at the turbine's entrance and, hence, the mechanical torque produced by the turbine.

TABLE I
Power System Data for Fig. 5

Parameter	Machine 1	Machine 2	Machine 3
Machine Data			
H (sec)	23.64	6.4	3.01
X_d (pu)	0.146	0.8958	1.3125
X'_d (pu)	0.0608	0.1198	0.1813
X_q (pu)	0.0969	0.8645	1.2578
X'_q (pu)	0.0969	0.1969	0.25
T'_{d0} (sec)	8.96	6.0	5.89
T'_{q0} (sec)	0.31	0.535	0.6
Governor Data			
K_P (pu)	100	100	100
K_I (sec^{-1})	15	15	15
K_D (sec)	0	0	0
D_r (pu)	0.06	0.06	0.06
R_D (pu)	0.05	0.05	0.05
T_g (sec)	0.2	0.2	0.2

B. Wicket Gate and Mechanical Power of the Turbine

The mechanical power provided by the turbine is converted into electrical power by the generator and delivered to the electrical load in the network. A simple power-consuming resistor R_0 connected to node 7 in Fig. 3 is used to represent this electrical power. R_0 is such that $P_{Mech} = V_7^2/R_0$, where V_7 is the hydraulic pressure (corresponding to the voltage in the equivalent circuit). When the wicket gate (that allows water into the turbine) is fully open, the electrical network uses the maximum power available, whereas when the wicket gate is fully closed, no mechanical power is available, and no electrical power goes into the network.

If we assume a linear relationship between the wicket gate position and the available mechanical power, then the power absorbed by the equivalent electric power-consuming resistor R_0 is directly proportional to the wicket gate position G_t, $P_{Mech} = T_M \omega_{pu} = V_7^2/R_0 = V_7^2\, G_t$, where $R_0 = 1/G_t$. The wicket gate position G_t is chosen to be 1.0 in per unit when the gate is fully open.

C. Electrical Machines Model

The generators can be modelled using the classical $d-q$ model of Fig. 6 [10]. The complex variables associated with this model are

$$I_i = Conj\left(\frac{P_{E\,i} + Q_{E\,i}}{V_i}\right) \quad (7)$$

$$E_i = V_i + jI_i\, X'_{d\,i} \quad (8)$$

$$\delta_i = Angle(E_i) \quad (9)$$

$$I_{d\,i} + jI_{q\,i} = I_i e^{-j(\delta_i - \frac{\pi}{2})} \quad (10)$$

$$I_{d\,i} = Real(I_i e^{-j(\delta_i - \frac{\pi}{2})}) \quad (11)$$

$$I_{q\,i} = Imm(I_i e^{-j(\delta_i - \frac{\pi}{2})}) \quad (12)$$

$$P_{E\,i} = V_i I_{d\,i} \sin(\delta_i - \theta_i) + V_i I_{q\,i} \cos(\delta_i - \theta_i) \quad (13)$$

$$Q_{E\,i} = V_i I_{d\,i} \cos(\delta_i - \theta_i) - V_i I_{q\,i} \sin(\delta_i - \theta_i) \quad (14)$$

where subscript i is the generator number, I_i is the

current, $P_{E\,i}$ is the active power, $Q_{E\,i}$ is the reactive power, V_i is the voltage, 9 is the internal voltage, $X'_{d\,i}$ is the transient d-axis reactance, all in pu and δ_i is the power angle of the generator in radians, $I_{d\,i}$ is the d axis current, $I_{q\,i}$ is the q axis current, θ_i is the phase angle of V_i in radians.

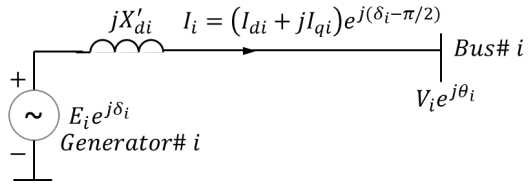

Fig. 6. Representation of each generator connected to the bus.

D. Power Flow Equations

The power flow equations for the balance of active and reactive power are

$$P_{E\,j} - V_j \sum_{k=1}^{9} V_k \left|Y_{jk}\right| \cos(\theta_j - \theta_k - \alpha_{jk}) = 0 \tag{15}$$

$$Q_{E\,j} - V_j \sum_{k=1}^{9} V_k \left|Y_{jk}\right| \sin(\theta_j - \theta_k - \alpha_{jk}) = 0 \tag{16}$$

where subscript j is the bus number, $P_{E\,j}$ and $Q_{E\,j}$ are the active and reactive power injected into the bus in pu, V_j are the voltages in pu, θ_j are the voltage phase angles in radians all at each bus and Y_{jk} are the admittance between each other bus and α_{jk} is the angle of the admittance Y_{jk}.

Equations (15) and (16) are solved using a Newton-Raphson iteration to determine the bus's voltages and phase angles. The power angles and the active and reactive power flow of each generator are determined by (7)-(14).

V. Case Studies

Four cases are presented using the IEEE nine-bus system of Fig. 5. Case A is a frequency stability study that compares the results, including the EMT-H equations and the conventional results without the EMT-H equations. Case B compares the traditional gate droop governor controller with the modern power droop governor controller. Case C proposes a new hybrid droop controller. Case D introduces the concept of a companion plant for joint compensating control action. Note that the time step used in all the cases was 0.01 seconds and that all generators were in either gate droop or power droop together.

A. Frequency Stability

By using the conventional equations for machine acceleration, each generator can be written [10] as, where subscript i indicates the generator number,

$$\dot{\delta}_i = \omega_i - \omega_s \tag{17}$$

$$\frac{2H_i}{\omega_s}\,\dot{\omega}_i = T_{M\,i} - T_{E\,i} - D_{r\,i}(\omega_i - \omega_s) \tag{18}$$

$$\frac{T_{g\,i}}{K_{I\,i}R_{D\,i}}\ddot{G}_{t\,i} = -G_{t\,i} + Pc_i - \frac{1}{R_{D\,i}}\left(\frac{\omega_i}{\omega_s} - 1\right) - \frac{K_{P\,i}}{K_{I\,i}R_{D\,i}}\frac{\dot{\omega}_i}{\omega_s} - \left(\frac{1}{K_{I\,i}R_{D\,i}} + \frac{K_{P\,i}}{K_{I\,i}}\right)\dot{G}_{t\,i} \tag{19}$$

Here δ_i is the power angle in radians, ω_i is the rotational speed in radians per second, ω_s is the nominal synchronous rotational speed, H_i is the machine inertia constant in seconds, $T_{M\,i}$ is the mechanical torque in per-unit quantities, $T_{E\,i}$ is the electrical torque in per-unit quantities, $D_{r\,i}$ is the damping constant in Newton-meters per radian per second, $G_{t\,i}$ is the wicket gate position in per-unit quantities, $T_{g\,i}$ is the governor gate time constant in seconds, Pc_i is the governor power setpoint in per-unit quantities, $R_{D\,i}$ is the governor speed droop in per-unit quantities, $K_{P\,i}$ is the governor proportional gain, and $K_{I\,i}$ is the governor's integral gain.

In the machine acceleration equation (18), torque is used for both the mechanical power and the electrical power. To obtain the electrical torque from the electrical power, we divide by ω_i which is the mechanical velocity.

Equations (17) – (19) are converted to a set of state space equations, as shown in (21). The fourth-order Runge-Kutta (RK4) method is used to solve the state equations for the next time-step solution for δ_i, ω_i and $G_{t\,i}$. In most studies [10], the shaft mechanical torque $T_{M\,i}$ is simply assumed to be proportional to the wicket gate position $G_{t\,i}$, ignoring the water conduit dynamics,

$$T_{M\,i} = G_{t\,i} \tag{20}$$

With this assumption, the state space equation can be written as,

$$\dot{X} = AX + Bu \tag{21}$$

where $X = \begin{bmatrix} \delta_i \\ \omega_i \\ G_{t\,i} \\ \dot{G}_{t\,i} \end{bmatrix}$ u=$\begin{bmatrix} \omega_s \\ T_{E\,i} \\ P_{c\,i} \end{bmatrix}$.

Other studies [9] assume that the shaft mechanical torque $T_{M\,i}$ is related to the wicket gate position $G_{t\,i}$ using a first-order differential equation known as the classical water start time dynamic equation,

$$T_{M\,i} = \frac{1 - T_w s}{1 + 0.5T_w s}\,G_{t\,i} \tag{22}$$

where T_w is the water starting time, which is a function of the length and the cross-sectional area of the water conduit. The associated differential equation is

$$0.5T_w\,\dot{T}_{m\,i} = -T_{M\,i} + G_{t\,i} + T_w\dot{G}_{t\,i}. \tag{23}$$

With this equation, the mechanical torque $T_{M\,i}$ becomes a time-dependent state variable, and the state space vector of (21) becomes $X = [\delta_i\ \omega_i\ G_{ti}\ \dot{G}_{ti}\ T_{Mi}]^T$.

Combining the differential equations from the state space formulation (21) and the algebraic equations from (13) - (16), we obtain a system of Differential Algebraic Equations (DAE) [10] that is solved by iterations. Fig. 7 below shows a flow chart of the solution process that includes the hybrid of the EMT-H (in red). The initial conditions are obtained with a steady-state power flow solution, where the electrical and mechanical

torques are in equilibrium. We iterate the power flow equations using the Newton-Raphson method and solve the hydraulic equations sequentially with the EMT-H model, as shown in Fig. 7 in red.

Fig. 8 shows the simulation results using (20), where the water conduit dynamics are ignored and using (22), where the water start-time conduit dynamics are included in the conventional way. It can be seen that the system frequency dynamics are significantly different in these two cases. In particular, if we ignore the water dynamics, the results do not show the inter-area oscillations.

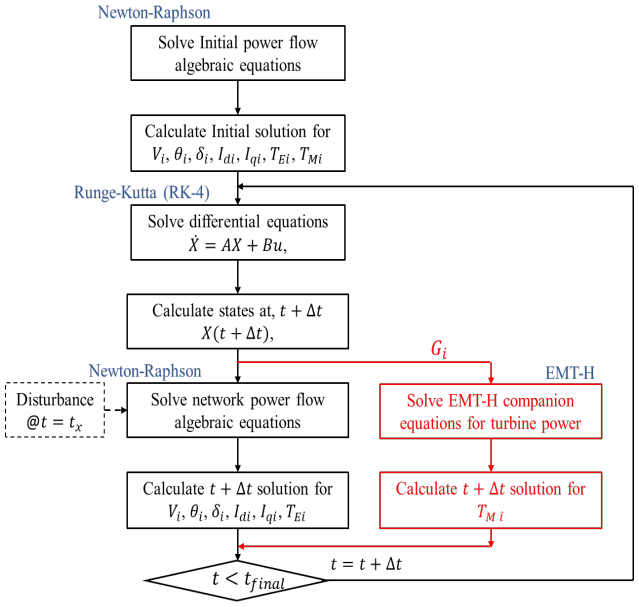

Fig. 7. EMT-H / DAE Hybrid Solution flowchart.

When the proposed EMT-H model is used, the results are significantly different from those of the traditional models (Fig. 8 red and green traces). These errors significantly affect the nadir point of the response and the steady-state settling point. The single time constant in (22) cannot accurately represent the true travelling wave nature of the pressure dynamics or the power loss along the water conduit.

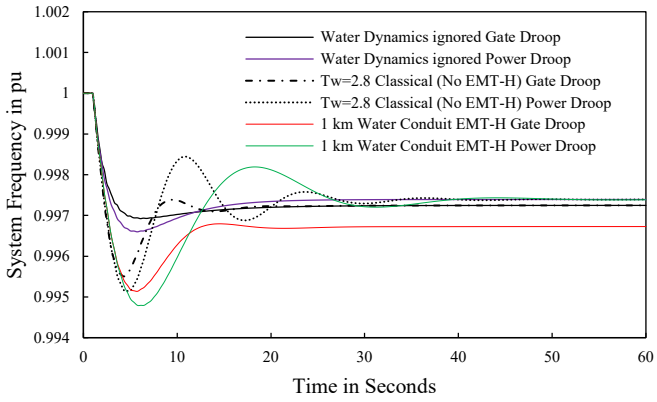

Fig. 8. IEEE nine-bus, three-machine power system frequency deviations to an electrical load step change, classical approach and EMT-H.

Fig. 10 below shows the effect of the conduit length on the results obtained with the EMT-H model. The solid trace corresponds to the classical case of (22) when the water start time T_w is taken as 2.8 seconds to represent 1 km water conduit. The EMT-H model shows that as the length of the conduit increases, the magnitude of the oscillations increases, and the length of the conduit should be considered in the control scheme to stabilize the system dynamics in the range of 0.02-0.05 Hz.

B. Gate Droop versus Power Droop Governors

In modern digital governors, power droop controllers are the preferred method to match the output electrical power with the input mechanical power (Fig. 9 with the switch selected to power droop position). This is called the power-droop method. The older electromechanical governors use the gate position for the droop feedback (Fig. 9 with the switch selected to gate droop position). This method is called the gate-droop method. A general droop controller is shown in Fig. 9, with the droop selection switched to the gate droop position.

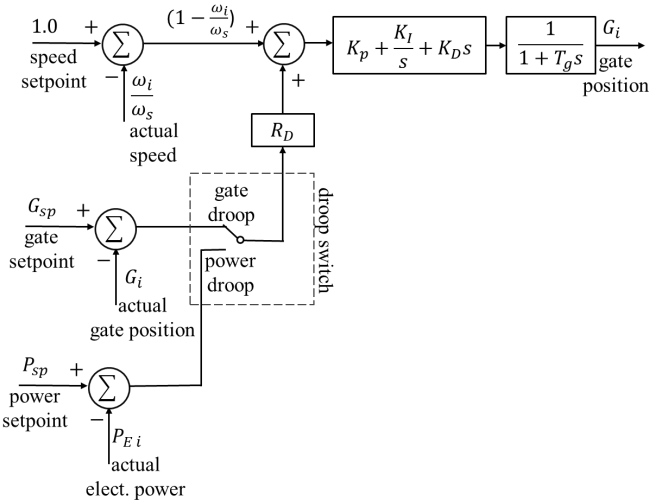

Fig. 9. Transfer function representation of the Governor model with power droop and gate droop.

In the gate droop control scheme, the gate position along the droop line is automatically changed based on the frequency of the power system. Power-droop governors also indirectly change the gate position, but in this case, the gate position is moved until the active power needed is reached along the droop line.

In this work, we postulate that by including the hydraulic flow dynamics in the control scheme, better control of the system frequency can be achieved using traditional gate-droop controllers than modern power-droop controllers. In modern power-droop controllers, heavy filtering of the measured electrical active power signal is performed. Although this filtering seems beneficial in eliminating unwanted gate movements, it inherently adds a significant time delay to the governor's response.

Fig. 10 compares the response of power-droop and gate-droop controllers for a step load increase. In terms of the nadir frequency point, the gate-droop governor shows a 40% lower drop in frequency compared with the power-droop governor. In terms of settling time, the gate-droop gives more than 30%

improvement compared to the power-droop governor in the case where the water conduit length is 0.5 km. As the water conduit length increases, the advantages of the gate-droop controller increase significantly.

As can be seen in Fig. 10 (b), the power-droop governors have the advantage of converging to the system's steady state frequency for different water conduit lengths, as the active power feedback compensates for the power loss along the water conduit. The gate-droop controllers, however, do not settle at the same steady state frequency without supplementary control (Fig. 10 (a)). In our opinion, though, this is a small issue that can be easily corrected using secondary frequency control compared to the advantages of the gate-droop controller's better transient response.

Note, also, that the classical water time-constant model of (22) ignores the water conduit losses, while the EMT-H model considers these losses correctly during the transient.

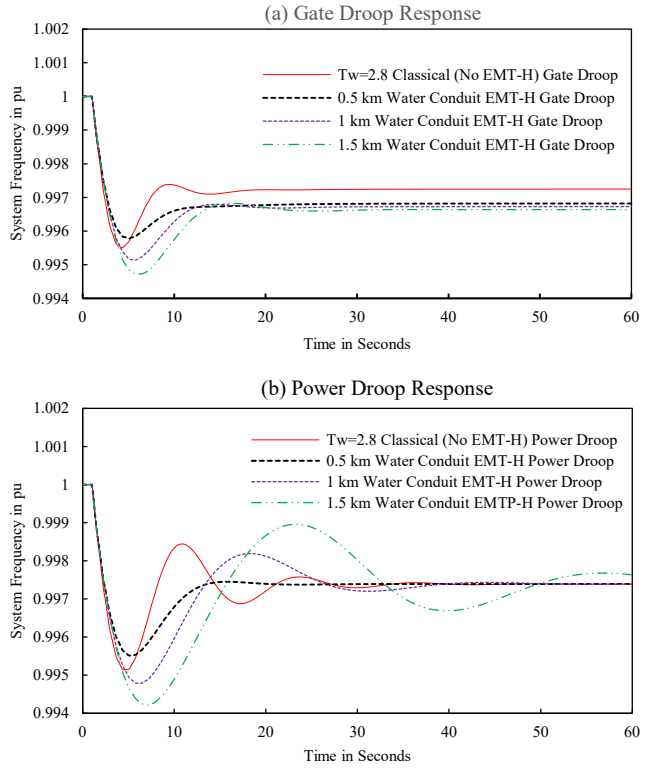

Fig. 10. Combined EMT-H and DAE models for different water conduit lengths for (a) Gate Droop and (b) Power Droop.

C. Proposed Hybrid Droop Governor Controller

Next, we propose a hybrid droop governor that combines the advantages of power droop and gate droop controllers. This controller is shown in Fig. 11. In this controller, the governor droop feedback signal is modified to act as a "gate droop" during the transient and a "power droop" after settling to a steady state using a low pass filter.

Fig. 12 shows the results obtained in our test case using the proposed Hybrid Gate/Power droop controller. These results show the advantages of the gate droop controller in improving the frequency nadir while maintaining the advantage of the power droop in settling to the steady-state frequency. The filter time constant (T_F in Fig. 11) should be chosen so that the frequency excursions are dampened to an adequate amount. Given these results, we recommended that the power droop mode be changed to gate droop mode for existing digital governors. Similarly, we recommend that the proposed hybrid controller be used for new digital governor installations.

D. The remote EMT-H compensator

The EMT-H local compensator, as shown in Fig. 13, dampens the oscillations and improves the nadir point. However, it makes the overall governor slower to respond. This sluggishness is due to the compensating signal acting as a transient gain reduction of the governor controller. Using the EMT-H model's capability of predicting hydraulic pressure transients in real-time, we can introduce the concept of using a remote plant (preferably a plant with short water conduits or a steam or gas plant) to assist in improving the local hydraulic plant oscillations. The proposed scheme is shown in Fig. 14, where a feed-forward signal is sent to the remote plant to obtain its assistance in our control loop.

For our example system (generator 1 with a 1 km long water conduit as the local plant and generator 2 with a 10 m long water conduit as the remote plant), Fig. 15 shows the improvement in the response of the system frequency to a step change in load implementing the remote plant compensating scheme.

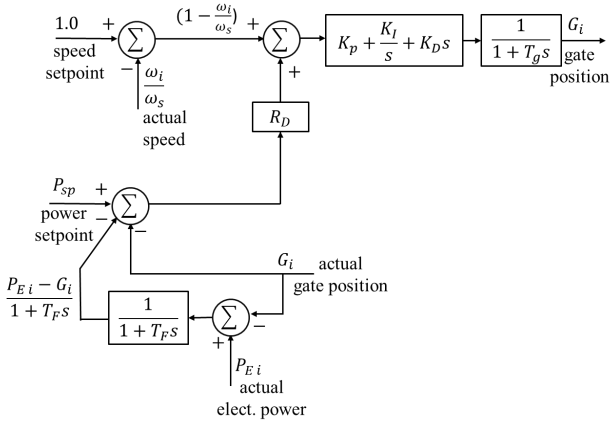

Fig. 11. Proposed Power/Gate Hybrid droop governor model.

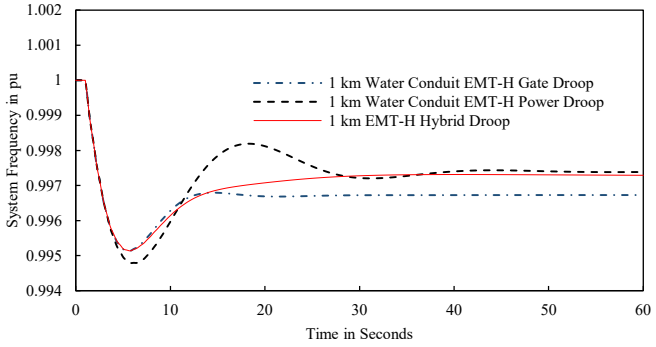

Fig. 12. Comparison of Power Droop, Gate Droop and Hybrid Droop.

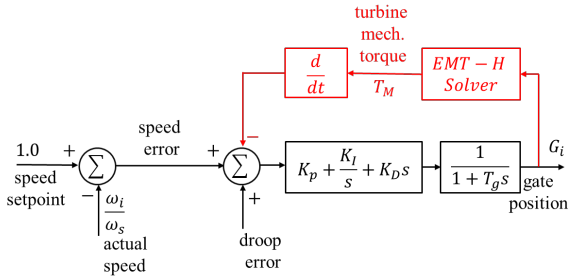

Fig. 13. Local EMT-H compensator to complement the hydraulic transients of local hydro plant with long conduit.

One aspect to consider in this scheme is the communications time needed by this remote-control signal. This effect has been included in the results of Fig. 15. As long as the signal delay is less than the wave travelling time, which is typically in the range of seconds, the communications delay has little influence on the effectiveness of the compensation.

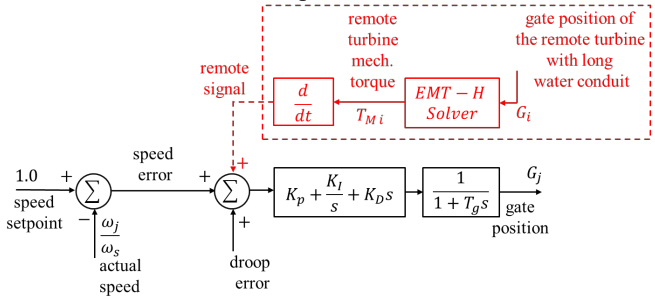

Fig. 14. Remote EMT-H compensator for the conjugate gas turbine plant (or hydro plant with short water conduit) to complement the hydraulic transients of local hydro plant with long conduit.

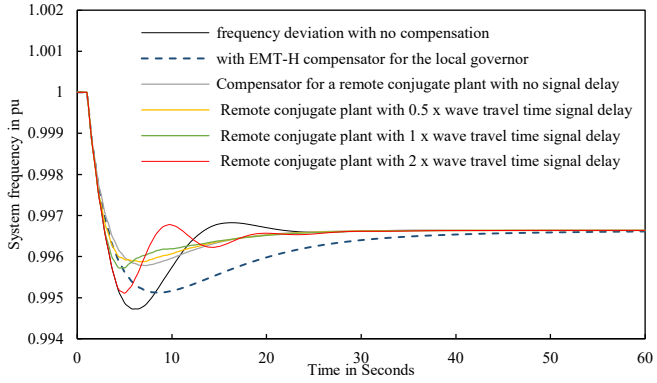

Fig. 15. Comparison of results with local EMT-H compensator and remote conjugate plant EMT-H compensator with different signal transmission delays.

VI. Conclusions

This paper has discussed the effect of considering the water hydraulic dynamics in the water conduits of hydro generation plants during dynamic transients in the electrical part of the power system. Due to the length of the conduits of some of these plants, these dynamics can have a strong influence and the results obtained with the traditional models are not accurate enough.

To model the water dynamics, we use the EMT-H model, which implements the water propagation equations using companion EMT transmission line models.

The EMT-H model is much faster than traditional finite-difference solutions classically used for hydraulic transients (two orders of magnitude in the cases considered in this paper) and can be used in the control loop of real-time governor controllers to improve the frequency dynamics of the electrical network.

A number of case studies are presented that show how the water dynamics, together with the governor controller, affect the frequency transients in the power system. By including the EMT-H equations in the control loop, it is shown that the performance of gate-droop controllers is better than the currently preferred power-droop controllers. This is particularly noticeable when the water conduit lengths are relatively long. A hybrid controller is proposed that combines the better transient performance of gate-droop controllers with the capability of power-droop controllers to settle at the steady state frequency point.

In the paper, we also introduced the concept of using a companion remote plant (thermo-plant or hydro-plant with short water conduits) to provide a stabilization signal to our long-water-conduits local plant to increase its momentary power support to the electrical system. This signal is obtained from the EMT-H model and is applied as a supplementary control signal to the external unit's governor.

VII. References

[1] H. Chaudhary, Applied Hydraulic Transients, 3rd ed, Springer ISBN 978-1-4614-8537-7, 2014, pp. 36-109.

[2] A.R. Halliwell, "Velocity of a Water Hammer Wave in an Elastic Pipe", American Society of Civil Engineers, Journal of Hydraulics Engineering, vol. 89, No. HY4, July, pp.1-21, 1963.

[3] R. Mutukutti, and J.R. Marti, "Modelling of Water Conduit Dynamics Using the Electromagnetic Transient Program Line Model," in Proc. 22nd Power Systems Computation Conference, Porto Portugal, Electric Power Systems Research, vol. 212, November 2022, p. 108401.

[4] H.W. Dommel, "Digital Computer Solution of Electromagnetic Transients in Single and Multiphase Networks", IEEE Trans. Power Apparatus and Systems, Englewood Cliffs, N. J., PAS-88(4), pp. 388-399, 1969.

[5] R. Fitzgerald, and V.L. Van Blaricum, Water Hammer and Mass Oscillation (WHAMO) 3.0 user manual, US Army Cope of Engineers Construction Engineering Research Laboratories USACERL ADP Report 98/129, 1998.

[6] Hermann W. Dommel, EMTP Theory Book, 2nd ed, Microtran Power Systems Analysis Corporation, Vancouver BC, 1996.

[7] J. R. Martí, "Accurate modelling of frequency-dependent transmission lines in electromagnetic transients simulations," IEEE Transactions on Power Apparatus and Systems, vol. 1, pp. 147-157, 1982.

[8] F. Sadeque, and J. Taylor, 12th international conference on pressure surges, Dublin, Ireland, 2015, pp. 405-415.

[9] P. Kundur, Power system stability and control, New York, McGraw-Hill, 1993, pp.379-418.

[10] Peter W. Sauer, and M. A. Pai, Power system dynamics and stability, The University of Illinois, Urbana, IL 61801, 2007, pp.155–211.

[11] X. Liu, and C. Liu, "Eigen Analysis of Oscillatory Instability of a Hydro Plant Including Water Conduit Dynamics", IEEE Transactions on Power Systems, vol. 22, no.2, pp. 675–681, 2007

[12] Working Group on Prime Mover and Energy Supply Models for System Dynamic Performance Studies "Hydraulic turbine and turbine control models for system dynamic studies," IEEE Transactions on Power Systems, vol. 7, no.1 pp. 167–179,1992.

[13] O. H. Souza, Jr, N. Barbieri, and A. H. M. Santos, "Study of hydraulic transients in hydropower plants through simulation of nonlinear model of penstock and hydraulic turbine model," IEEE Transactions on Power Systems, vol. 14, no.4 pp. 1269–1272, Nov.1999.

[14] R. A. Naghizadeh, S. Jazebi, and B. Vahidi, "Modeling Hydro Power Plants and Tuning Hydro Governors as an Educational Guideline",

International Review on Modelling and Simulations, Vol. 5, No.4 August 2012.
[15] H. Kim, and S. Kim, “A Generalized Procedure for Pipeline Hydraulic Components in Quasi-Two-Dimensional Unsteady Flow Analysis” Journal of Fluids Engineering, Vol. 141, p. 061107, June 2019.
[16] S. Kim, “Holistic Unsteady-Friction Model for Laminar Transient Flow in Pipeline Systems”, Journal of Hydraulic Engineering, pp. 1649-1657, December 2011.
[17] C. Wang, and J. Yang, “Water Hammer Simulation Using Explicit-Implicit Coupling Methods”, Journal of Hydraulic Engineering, p. 04014086, Vol. 141(4), 2015.